

Highlights

Design of universal chemical relaxation oscillator to control molecular computation

Xiaopeng Shi, Chuanhou Gao

- We give an approach of designing universal chemical oscillator for synchronous sequential computation in biochemical systems.
- We analyse the properties of the oscillator model in detail, such as period and amplitude, as well as the dynamic behaviour under different parameter values.
- We test the adjustment performance of our chemical oscillator based on the counting model.
- We give a method for the system to terminate the loop spontaneously.

Design of universal chemical relaxation oscillator to control molecular computation[★]

Xiaopeng Shi^a, Chuanhou Gao^{a,**}

^a*School of Mathematical Science, Zhejiang University, Hangzhou, 310000, , PR China*

ARTICLE INFO

Keywords:

chemical oscillator
relaxation oscillation
synchronous sequential computation
chemical reaction network

ABSTRACT

Embedding efficient command operation into biochemical system has always been a research focus in synthetic biology. One of the key problems is how to sequence the chemical reactions that act as units of computation. The answer is to design chemical oscillator, a component that acts as a clock signal to turn corresponding reaction on or off. Some previous work mentioned the use of chemical oscillations. However, the models used either lack a systematic analysis of the mechanism and properties of oscillation, or are too complex to be tackled with in practice. Our work summarizes the universal process for designing chemical oscillators, including generating robust oscillatory species, constructing clock signals from these species, and setting up termination component to eventually end the loop of whole reaction modules. We analyze the dynamic properties of the proposed oscillator model in the context of ordinary differential equations, and discuss how to determine parameters for the effect we want in detail. Our model corresponds to abstract chemical reactions based on mass-action kinetics which are expected to be implemented into chemistry with the help of DNA strand displacement cascades. Our consideration of ordering chemical reaction modules helps advance the embedding of more complex calculations into biochemical environments.

1. Introduction

A main desire of synthetic biology is designing programmable chemical controller which can operate in molecular contexts incompatible with traditional electronics [1]. We have learned plenty of algorithms from how life works such as artificial neural network and genetic algorithm, while on the contrary, inserting advanced computational methods into living organisms to accomplish specific tasks e.g. biochemical sensing and drug delivery is also fascinating. A great deal of related work has sprung up in recent years: Moorman et al. proposed a biomolecular perceptron network in order to recognize patterns or classify cells *in-vivo* [2]. The beautiful work of Vasic et al. put the feed-forward RRelu neural network into chemical reaction networks(CRNs), and performed their model on standard machine learning training sets [3]. There were also some attempts to build CRNs capable of learning [4, 5]. However, no one has implemented the whole neural network computation(including feed-forward and parameter-learning process) into biochemical system. The main reason is that algorithm based on computer instruction performs operations in a sequential manner whereas biochemical reactions proceed synchronously. This contradiction calls for an appropriate mediation method, which isolates two reaction modules [1] from co-occurring and controls their order. D Blount et al. constructed cell-like compartments and added clock signals artificially in order to solve this problem, which increased the difficulty of biochemical implementation [5]. A more natural idea

is to design chemical oscillators which produce periodical clock signals automatically, taking advantage of their phase change to turn corresponding reaction module on or off.

Oscillation phenomena are often encountered in chemical and biological systems such as Belousov-Zhabotinskii reaction [6] and circadian rhythm [7], while dealing with reaction orders by chemical oscillators is not a groundless rumour. Arredondo and Lakin [8] utilized a 20-dimensional oscillator extended from ant colony model [9] to order the parts of their chemical neural networks. Jiang et al. introduced a different oscillator model with 12 species and 24 reactions [10], then chose two of these species to serve as clock signals. Their work follows the same logic: Firstly, find a suitable oscillator model and give a set of appropriate parameters(along with initial values), then confirm that the model is indeed available for use by simulation. There are two main problems with such design, one is the lack of theory about oscillation mechanism i.e. it is often unclear why these models produce oscillatory behaviour. The other one is that these oscillators belong to harmonic type, whose amplitude and period may not recover the initial values after a perturbation. In order to obtain a satisfactory oscillator structure, these models are highly required to select accurate initial values, which causes difficulties during biochemical implementation. In view of this, we consider to design a set of oscillator models based on transparent mechanism, making sure why the oscillation behavior occurs and how it evolves are clear, and selection of initial values is robust. We also give the relationship between period and parameters in our oscillator model.

Our ultimate goal is to perform our chemical oscillator *in-vivo* together with other operational modules based on chemical reactions, so concentrations of chemical species play the role in our oscillator model. The whole process consists of three steps: construct oscillator model in the

[★]This work was funded by the National Nature Science Foundation of China under Grant No. 12071428 and 62111530247, and the Zhejiang Provincial Natural Science Foundation of China under Grant No. LZ20A010002.

^{**}Corresponding author

✉ 12035033@zju.edu.cn (X. Shi); gaozhou@zju.edu.cn (C. Gao)
ORCID(s):

context of dynamical system first, then select the appropriate kinetics (mainly mass action kinetics) to put it back into abstract chemical reaction networks [11], and finally utilize DNA strand displacement cascades [12] to implement them into chemistry. Since each step of the above transformation process has a relatively mature theory as a guarantee, it is reasonable to carry out our work on the theoretical level of ODE and dynamical system.

We focus on designing chemical oscillators for the sequence of two chemical reaction modules and making sure that our method is still valid when faced with the task of ordering multiple reaction modules. Both controlling the sequence and alternating cycles of two reaction modules are very common in molecular operations and synthetic biology, such as module instructions that involve judgment before execution, or reaction modules that realize the loop of feed-forward transmission and back propagation in artificial neural networks. Not only do we provide a common approach of designing transparent oscillator for such requirements, but we also offer a method for how to let the modules terminate the loop according to the judgment statement spontaneously.

This paper is organized as follows. Related definitions are given in section II. Section III exhibits the structure of 4-dimensional universal oscillator model based on 2-dimensional relaxation oscillation, which is able to generate a pair of desired oscillatory component with proper selection of parameters. In section IV the dynamical behaviours involved in this model are analyzed in detail, and the amplitude and period of oscillatory components are estimated with appropriate parameter values. Then we talk about ways to make the system spontaneously terminate the loop in section V. We summarize the general process of placing our oscillator components into reaction modules to be ordered with example of chemical neural network in section VI. And finally, section VII is dedicated to conclusion and discussion of the whole paper.

2. Related definitions

In this section we provide the preparatory knowledge such as definition and concept of chemical reaction network first, following the work of Feinberg [11] and Anderson et al [13]. Then based on our example of our reaction modules, we talk about the design requirements for chemical oscillators.

2.1. fundamental concept of chemical reaction network(CRN)

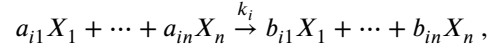
Definition 2.1 A chemical reaction network(CRN for short) consists of nonempty and finite set of species S and finite set of complexes C and set of reactions \mathcal{R} satisfying the following description:

- * Elements of species S act as fundamental components in CRN.
- * Every complex in C is a linear combination of species over the non-negative integers.

* Two complexes connected by arrow form a reaction belonging to \mathcal{R} .

* Species to the left of the arrow in each reaction are called reactants for that reaction, and the species to the right are called products.

We often denote the species set as $S = \{X_1, \dots, X_n\}$, in which case the complexes are of the form $a_1 X_1 + \dots + a_n X_n$, where $a_i \in \mathbb{Z}_{\geq 0}$ for each $i \in \{1, \dots, n\}$. Then the reaction set $\mathcal{R} = \{R_1, \dots, R_m\}$ and R_i is just like

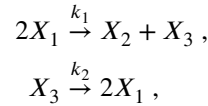


for k_i is the rate constant of this reaction. Based on different kinetic assumptions, we can model ordinary differential equations(ODEs for short) for species concentration changes according to a given chemical reaction network. This paper chooses the most common form of kinetics termed *mass-action kinetics*:

$$\dot{x} = \Gamma \cdot v(x).$$

In which $x \in \mathbb{R}_{\geq 0}^n$ represents the concentration of species X_1, \dots, X_n , coefficient matrix $\Gamma_{n \times m}$ satisfies $\Gamma_{ij} = b_{ij} - a_{ij}$ and rate function $v(x) = (k_1 \prod_{i=1}^n x_i^{a_{i1}}, \dots, k_m \prod_{i=1}^n x_i^{a_{im}})^T$.

Example 2.1 Consider the following reaction system:



with the species set $S = \{X_1, X_2, X_3\}$, the complex set $C = \{2X_1, X_2 + X_3, X_3\}$, the stoichiometric matrix

$$\Gamma_{n \times m} = \begin{pmatrix} -2 & 2 \\ 1 & 0 \\ 1 & -1 \end{pmatrix} \text{ and the vector-valued rate function}$$

$v(x) = (k_1 x_1^2, k_2 x_3)^T$. The ODEs are

$$\begin{aligned} \frac{dx_1}{dt} &= -2k_1 x_1^2 + 2k_2 x_3, \\ \frac{dx_2}{dt} &= k_1 x_1^2, \\ \frac{dx_3}{dt} &= k_1 x_1^2 - k_2 x_3. \end{aligned}$$

Based on expression of ODEs, we give the definition of catalyst, which would be the form of the oscillatory component that we construct as clock signal participating in the reaction modules.

Definition 2.2 We call a species X_i catalyst of a specific CRN for that $\frac{dx_i}{dt} = 0$.

2.2. Reaction Modules in Molecular Calculation

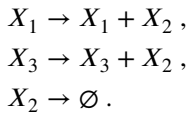
The concept of reaction modules comes from utilizing chemical reactions to perform operations [1, 14]. Consider the concentration of certain species at one time as the system input and concentration of certain species at another time as the output (input species and output species are usually different), chemical reaction networks can serve as a framework for calculation, and it has been proven that deterministic (mass-action) chemical kinetics is Turing universal [15].

There are, as far as we know, two main ways of constructing chemical reactions to achieve a specific operation: One is choosing non-competitive (NC) CRNs whose equilibria are absolutely robust to reaction rates and kinetic rate law [3], so reaction networks can always achieve specific results regardless of the influence of parameters and initial values. The other one is regarding the operation to be implemented as the expression of ODEs at the equilibrium point [1], what operation the reaction network implements depends on kinetic assumption, parameters and initial values of ODEs and even speed of convergence. Although the former has good robustness, it can realize a very narrow range of operations [16]. While the latter can perform general operations, requiring elaborate design. This paper precisely addresses the problem of coupling reaction modules designed by the latter.

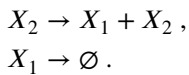
We first give an example about reaction modules:

Example 2.2

reaction module 1:



reaction module 2:



When the reaction rate constant is exactly 1, we omit it by default, and $X_i \rightarrow \emptyset$ refers to outflow reaction. Considering that the implementation of complex operations requires multiple reaction modules to be coupled, we command that the concentrations of species as input remain constant under the module operation. So in reaction module 1, both X_1 and X_3 are input species and species X_2 is output; while in reaction module 2, the input is X_2 and output is X_1 . Based on mass-action kinetics, we achieve the ODEs for the two reaction modules.

reaction module 1:

$$\begin{aligned} \frac{dx_1}{dt} &= 0, \\ \frac{dx_2}{dt} &= x_1 + x_3 - x_2, \\ \frac{dx_3}{dt} &= 0. \end{aligned} \quad (1)$$

reaction module 2:

$$\begin{aligned} \frac{dx_1}{dt} &= x_2 - x_1, \\ \frac{dx_2}{dt} &= 0. \end{aligned} \quad (2)$$

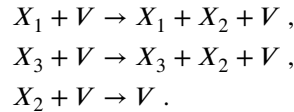
These modules correspond exactly to the description of Add module and Id module by Vasic et al. [1]. We let concentration of species X_3 play the role of constant value 1 (make its initial value equal 1), then the alternation of these two modules realizes the operation instruction like $x_1 + = 1$. However, if we just put these two reaction modules together, the concentrations of X_1 and X_2 would continue to increase to infinity without interruption, which fails to reach our aim. This is the stage for chemical oscillators.

2.3. Design requirements for chemical oscillators

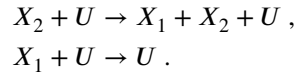
To be specific in our Example 2.2, we actually need to interrupt and stagger the progression of reactions in the two modules without changing the computational content of the respective module. So we construct two clock signals that are served by specific species U and V , and add them to the two separate modules as catalyst. Then we get modified reaction modules:

Example 2.3

modified reaction module 1:



modified reaction module 2:



Putting them together, the ODEs change:

$$\begin{aligned} \frac{dx_1}{dt} &= (x_2 - x_1)u, \\ \frac{dx_2}{dt} &= (x_1 + x_3 - x_2)v, \\ \frac{dx_3}{dt} &= 0. \end{aligned} \quad (3)$$

We naturally use u and v to refer to the concentrations of U and V . In order to shut down specific reaction module, concentration of the clock signal needs to stay near zero for some time, and then goes beyond zero to open the module again. Note that our ultimate goal is to have the two reaction modules alternating in cycles, and we treat this example as "Counter Model" which will be used for the spontaneous termination of loop. Then the oscillatory structures of clock signal U and V should exhibit a certain degree of symmetry. We conclude these as following definitions.

Definition 2.3 A species is called clock signal for that its concentration oscillates over time, which reaches zero or close enough during some part in a oscillation period and immediately goes beyond zero during the rest part.

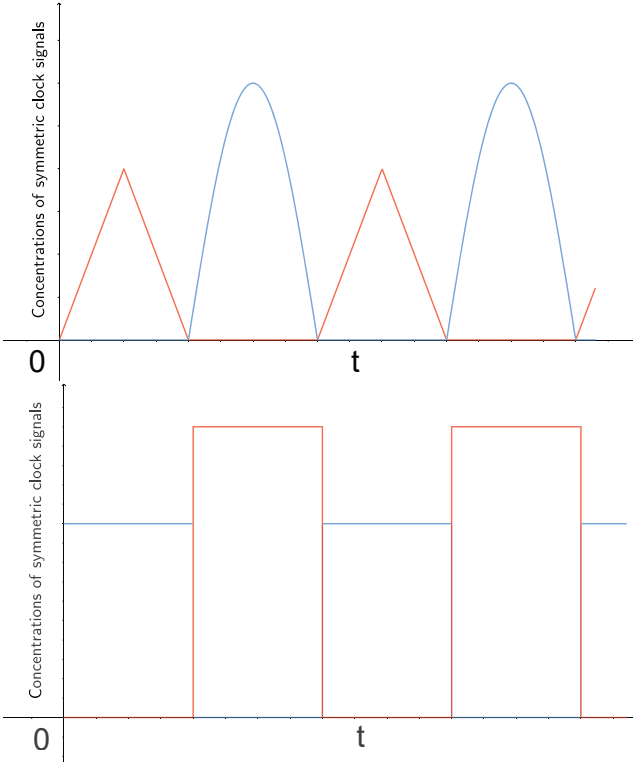


Figure 1: Two diagrams for symmetric clock signals.

Definition 2.4 A pair of clock signals U and V are called symmetric for that when U oscillates to zero or close enough, V goes strictly beyond zero, and vice versa.

We give two diagrams for symmetric clock signals in Fig.1.

Although the clock signals in both diagrams meet our expectations, We find that the former is more difficult to construct accurately than the latter. Concentrations of the two components will always cross at non-zero, leading to inevitable error. Our chemical oscillator can generate the latter form of clock signals, although they do not remain level at high amplitude, which does not affect the regulation of the reaction modules.

3. Universal Chemical Oscillator based on Relaxation Oscillation

This section we introduce the oscillation mechanism we choose and demonstrate its advantages for generating oscillator models. Note that advantages of our oscillator model are the transparency of mechanism and the independence of initial value selection, rather than independence of parameter selection.

3.1. 2-dimension Relaxation Oscillation

Although there are various mechanisms for generating oscillations [17, 18, 19, 20], few of them can reach our requirements. We give up harmonic oscillators whose oscillatory structure is highly sensitive to the selection of initial values. Most of the limit cycle oscillations we know

are difficult to produce oscillatory components that satisfy the definition of clock signals. So we choose relaxation oscillation as the basic mechanism for designing universal chemical oscillators.

Relaxation oscillation is a common type of oscillation in biochemical systems [21], which can be found from the Oregonator model [22] and the Fitzhugh-Nagumo model [23] in different contexts and its dynamic behaviour has been studied in detail [23, 24, 25]. We first give 2-dimensional structure of general relaxation oscillation model:

$$\begin{aligned} \epsilon \dot{x} &= f(x, y), \\ \dot{y} &= g(x, y), \end{aligned} \quad (4)$$

$$x \in \mathbb{R}, y \in \mathbb{R}, 0 < \epsilon \ll 1.$$

We give following hypothesis for the existence of relaxation oscillation adopted from [24].

Hypothesis 3.1 1. The critical manifold is defined by $S \stackrel{\text{def}}{=} \{(x, y) : f(x, y) = 0\}$ and it is S-shaped: Manifold S can be written in the form $y = \varphi(x)$ and the smooth function φ has precisely two extreme points, one non-degenerate minimum $x = x_m$ and one non-degenerate maximum $x = x_M$. The two points divide critical manifold S into three parts: S_l , S_m and S_r :

$$\begin{aligned} S_l &= \{(x, \varphi(x)) : x < x_m\}, \\ S_m &= \{(x, \varphi(x)) : x_m < x < x_M\}, \\ S_r &= \{(x, \varphi(x)) : x > x_M\}. \end{aligned}$$

2. S_l and S_r are attracting, i.e. $\frac{\partial f}{\partial x} < 0$ on S_l and S_r , while S_m is repelling, i.e. $\frac{\partial f}{\partial x} > 0$ on S_m .
3. Both extreme points satisfy conditions: $\frac{\partial^2 f}{\partial x^2}(x_0, y_0) \neq 0$, $\frac{\partial f}{\partial y}(x_0, y_0) \neq 0$, $g(x_0, y_0) \neq 0$.
4. The slow flow on S_l satisfies $\dot{x} > 0$ and the slow flow on S_r satisfies $\dot{x} < 0$.

Hypothesis 3.1 actually describes the phase plane portrait of system (4), which can be viewed as Fig.2. The coordinates of points are $A(x_A, y_M)$, $B(x_m, y_m)$, $C(x_C, y_m)$, $D(x_M, y_M)$. Then we define a singular trajectory Γ as $\Gamma = \{(x, y) \in S_l : x_A < x < x_m\} \cup \{(x, y_m) : x_m < x < x_C\} \cup \{(x, y) \in S_r : x_M < x < x_C\} \cup \{(x, y_M) : x_A < x < x_M\}$.

Lemma 3.1 Assume Hypothesis 3.1. Then for sufficiently small ϵ , there exists a unique limit cycle Γ_ϵ lying in a small tubular neighborhood of Γ . The cycle Γ_ϵ is strongly attracting and as $\epsilon \rightarrow 0$, the cycle Γ_ϵ approaches Γ in the Hausdorff distance.

This lemma is the famous result as THEOREM 2.1 in [24], applying Fenichel Slow manifold theory and fundamental knowledge of geometric singular perturbation can easily prove it, we do not repeat this here. Besides, M. Krupa et al. mentioned more complex issues such as canard explosion, brief appearance and disappearance of limit cycles caused by

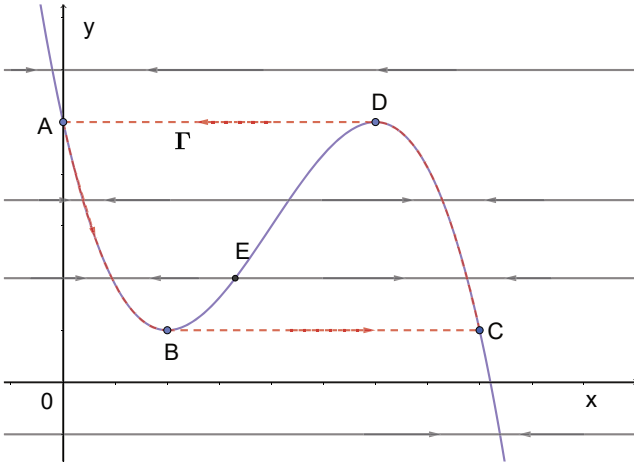


Figure 2: Phase plane portrait of system (4) based on Hypothesis 3.1.

Hopf bifurcation [24], which are not the focus of this paper. Actually we are just interested in existence and robustness of the limit cycle Γ_ϵ named relaxation oscillation.

Note that we value the oscillatory components in terms of concentrations of species, so the limit cycle Γ_ϵ should be limited in the first quadrant of phase plane portrait. And for the convenience of designing oscillator, we also limit function g as linear function $g(x, y) = x + \mu y + \lambda$, $\mu \in \mathbb{R}$, $\lambda \in \mathbb{R}$.

Lemma 3.2 Assume the Hypothesis 3.1 and $g(x, y) = x + \mu y + \lambda$, $\mu \in \mathbb{R}$, $\lambda \in \mathbb{R}$, then system(4) has and only has equilibrium points on the manifold S_m . Moreover, we suppose that $\mu \leq 0$ and $|\mu|$ is small enough, then system(4) can only have one unique equilibrium point E , and E is unstable.

Proof The last one in Hypothesis 3.1 says that $\dot{x} > 0$ on S_l and $\dot{x} < 0$ on S_r while $\dot{x} = \frac{g(x, \varphi(x))}{\varphi'(x)}$. The sign of $\varphi'(x)$ on S_l is same as the one on S_r , so the graph of $g(x, y) = 0$ must be between S_l and S_r , which leads to equilibrium points on S_m . While equilibrium points on S_l or S_r would destroy the consistent result of the last one in Hypothesis 3.1, system(4) has and only has equilibrium points on S_m .

Moreover, suppose that $\mu \leq 0$ and $|\mu|$ is small enough, then system(4) has a unique equilibrium point E , and E must lie on manifold S_m . We define the part of S_m below E as S_{mb} , and the part above E as S_{ma} . Then the sign of $g(x, \varphi(x))$ on S_{mb} is same as the one on S_l , while signs of $\varphi'(x)$ are different. So the sign of \dot{x} on S_{mb} is negative. Similarly, $\dot{x} > 0$ on S_{ma} . This means that initial points close to E on S_m would stay away from E . Combined with the second one in Hypothesis 3.1, equilibrium point E is unstable. ■

Based on Hypothesis 3.1 and $g(x, y) = x + \mu y + \lambda$, system(4) can actually have odd equilibrium points on S_m , which would cause strange dynamics and complicate model analysis. However, our focus is not to analyze the dynamical properties of system(4) in any case. We limit g as linear

function along with range of parameter μ in order to simplify complexity of our oscillator model and achieve the desired dynamic behaviour.

We conclude Theorem 3.1 as follows:

Theorem 3.1 Assume Hypothesis 3.1 and add that:

1. Singular trajectory Γ with its small tubular neighborhood U strictly lies in the first quadrant.
2. $g(x, y) = x + \mu y + \lambda$, $\mu \leq 0$ and $|\mu|$ is small enough.

Then for sufficiently small ϵ , relaxation oscillation exists in the first quadrant of phase plane portrait and furthermore, all of trajectories starting from this quadrant except the equilibrium point reach the limit cycle Γ_ϵ finally.

Proof Lemma 3.1 ensures the existence of Γ_ϵ , which is closely related to the slow manifold. In Fenichel Slow Manifold Theorem [26], slow manifold M_ϵ falls in the $O(\epsilon)$ neighborhood of normal hyperbolic manifold M . So cycle Γ_ϵ can be viewed as perturbation of trajectory Γ under parameter ϵ . For sufficiently small ϵ , the relaxation oscillation Γ_ϵ approaches Γ in the Hausdorff distance and exists in the first quadrant. Lemma 3.2 shows that the invariant set of system(4) consist of singular trajectory Γ_ϵ and equilibrium point E . While E is unstable, the unique stable invariant set in first quadrant is Γ_ϵ . As is shown in Fig.2, trajectory with initial points on $S_l \cup S_r$ or nearby goes along the cycle Γ_ϵ immediately, while trajectory with initial points somewhere else in the first quadrant except E pours along horizontal flows at the beginning until reaching neighborhood of S_l or S_r , then oscillating along Γ_ϵ . So all of trajectories starting from first quadrant reach the limit cycle Γ_ϵ finally. ■

The sufficiently small parameter ϵ leads to two time scales in system(4), and Theorem 3.1 is actually the classical conclusion of fast-slow system. The main contribution of ϵ is making trajectory with initial points away from the neighborhood of S_l or S_r converge to left part or right part of Γ_ϵ quickly, which results in abrupt transitions between the phases of x .

Note that we show the independence between relaxation oscillation structure and initial value selection. However, we would not talk about robustness associated with parameters except ϵ which may exist in system(4), for that properties of oscillation such as amplitude and period are strictly dependent on these parameters.

We give an example with the form of relaxation oscillation based on system(4).

Example 3.1

$$\begin{aligned} \frac{dx}{dt} &= (-x^3 + 6x^2 - 9x + 5 - y) / \epsilon, \\ \frac{dy}{dt} &= x - 2. \end{aligned} \quad (5)$$

It is easy to verify that choice of function f and g satisfies the assumptions of Theorem 3.1, with $\epsilon = 0.001$ and initial point(1, 1), we get the simulation result in Fig.3. In the previ-

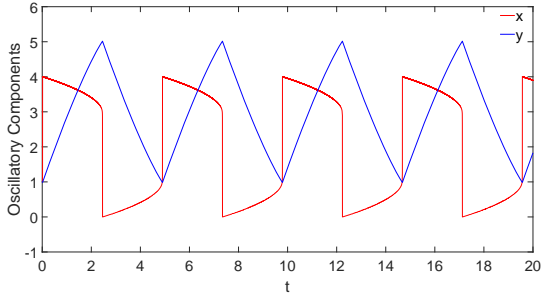


Figure 3: Simulation result of system(5)

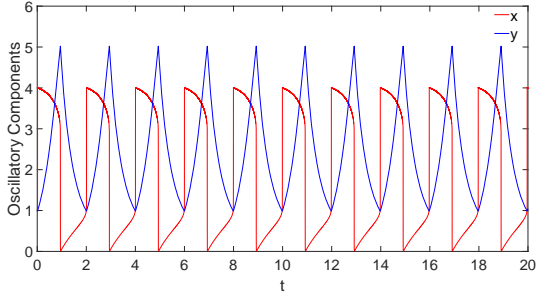


Figure 4: Simulation result of system(6)

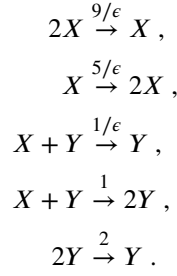
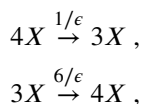
ous section we have shown how to use mass-action kinetics to model chemical reaction networks as ODEs. However, not all forms of ODEs can be converted back into chemical reactions [27]. In simple terms, if there is a negative term in the ODE expression corresponding to x , the value of x will decrease, then the species X corresponding to the chemical reactions should exist as the reactant (note that \dot{x} refers to concentration of species X). Therefore, the negative term in the ODE expression corresponding to x must factor in x . Example 3.1 actually makes no sense in CRN. Given this, we modify the functions in Example 3.1 as following:

Example 3.2

$$\begin{aligned} \frac{dx}{dt} &= (-x^3 + 6x^2 - 9x + 5 - y)x/\epsilon, \\ \frac{dy}{dt} &= (x - 2)y. \end{aligned} \quad (6)$$

Although the modification does not destroy the structure of critical manifold, two additional equilibrium points $(0, 0)$ and $(x_0, 0)$ ($-x_0^3 + 6x_0^2 - 9x_0 + 5 = 0$) emerge, which are saddle points. We just have to avoid the points on the axes as initial values, then Theorem 3.1 still holds. With the same values of parameter and initial point as Example 3.1, we give the simulation for Example 3.2 in Fig.4.

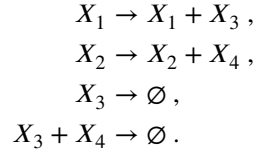
We supplement the corresponding CRNs as follows:



Note that our goal is to find a simplest model which can generate a pair of symmetric clock signals as we define in previous section based on relaxation oscillation, but the oscillatory components in system(4) can not reach our requirement for that neither x nor y could stay near zero enough for some time and they are not actually symmetric. So we need to use the oscillatory structure of x to construct new pair of components to act as symmetric clock signals by coupling x unidirectional to the module we will introduce next.

3.2. Coupled with Modified Truncated Subtraction Module

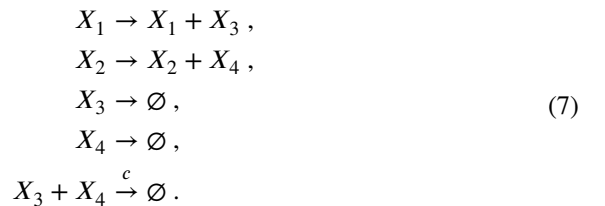
We first introduce the truncated subtraction module mentioned in [14, 1]:



which computes truncated subtraction corresponding to equilibrium of ODEs:

$$x_3 = \begin{cases} x_1 - x_2, & \text{if } x_1 > x_2 \\ 0, & \text{otherwise} \end{cases}$$

Based on this, we add the outflow reaction of species X_4 and consider the influence of reaction rate of the last reaction in order to treat output species X_3 and X_4 as our symmetric clock signals:



ODEs of reaction network(7) express as follows:

$$\begin{aligned} \frac{dx_3}{dt} &= x_1 - x_3 - cx_3x_4, \\ \frac{dx_4}{dt} &= x_2 - x_4 - cx_3x_4. \end{aligned} \quad (8)$$

Take x_1 and x_2 as inputs, if we value parameter c as zero i.e. species X_3 does not couple with X_4 , then reaction network (7) just load value of x_1 and x_2 separately into x_3 and x_4 . The

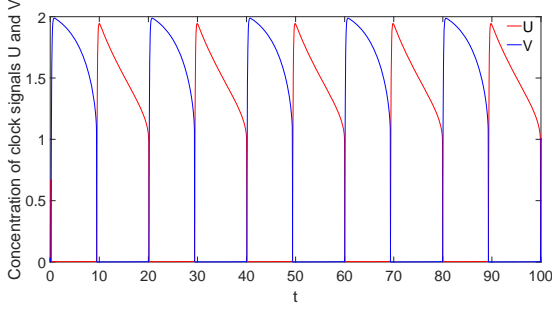


Figure 5: Simulation result of system(10)

coupling parameter c complicates the dynamic behaviour that the ODEs (8) can induce, which we would analysis in detail in next section.

Till now, we conclude our universal oscillator model in the context of ODEs:

$$\begin{aligned} \frac{dx}{dt} &= \eta_1 \eta_2 (f(x) - y)x/\epsilon, \\ \frac{dy}{dt} &= \eta_1 \eta_2 (x + \mu y + \lambda)y, \\ \frac{du}{dt} &= \eta_2 (p - u - cuv), \\ \frac{dv}{dt} &= \eta_2 (x - v - cuv). \end{aligned} \quad (9)$$

Where ODEs of x and y are just combination of system (4) and assumptions in Theorem 3.1 and the requirement for transformation from ODEs to CRNs, and we couple the expression of relaxation oscillation on x with modified truncated subtraction module (8): Substitute input species x to x_2 and utilize a constant p as x_1 . Parameters η_1 and η_2 are used to regulate the period of variables and can be inserted into corresponding reaction rates in CRNs.

We treat the value of u and v as the output and come back to Example 3.2 to show that corresponding species U and V could act as symmetric clock signals that we want.

Example 3.3

$$\begin{aligned} \frac{dx}{dt} &= \eta_1 \eta_2 (-x^3 + 6x^2 - 9x + 5 - y)x/\epsilon, \\ \frac{dy}{dt} &= \eta_1 \eta_2 (x - \rho)y, \\ \frac{du}{dt} &= \eta_2 (p - u - cuv), \\ \frac{dv}{dt} &= \eta_2 (x - v - cuv). \end{aligned} \quad (10)$$

With $\eta_1 = 0.01$, $\eta_2 = 10$, $\epsilon = 0.001$, $\rho = 2$, $p = 2$, $c = 400$ and initial point $(1, 1, 0, 0)$, we get simulation result as Fig.5.

Furthermore, return to the modified reaction module 1 and modified reaction module 2 in Example 2.3 and combine ODEs in system (3) and Example 3.3, we rewrite the whole

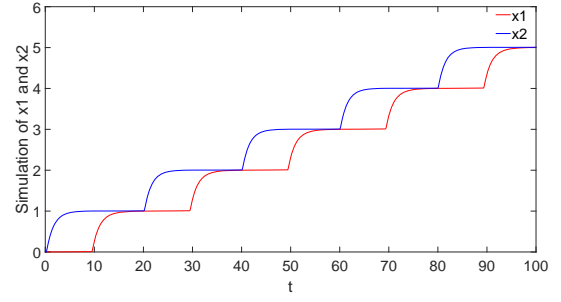


Figure 6: Simulation result of the Counter Model with components x_1 and x_2

ODEs as follows:

$$\begin{aligned} \frac{dx}{dt} &= \eta_1 \eta_2 (-x^3 + 6x^2 - 9x + 5 - y)x/\epsilon, \\ \frac{dy}{dt} &= \eta_1 \eta_2 (x - \rho)y, \\ \frac{du}{dt} &= \eta_2 (p - u - cuv), \\ \frac{dv}{dt} &= \eta_2 (x - v - cuv), \\ \frac{dx_1}{dt} &= \eta_3 (x_2 - x_1)u, \\ \frac{dx_2}{dt} &= \eta_3 (x_1 + 1 - x_2)v. \end{aligned} \quad (11)$$

We add another parameter η_3 to the last two equations in order to ensure the accuracy of adjustment by species U and V , and substitute the concentration of catalyst X_3 just as constant one. Choose $\eta_3 = 0.35$ and initial values of both x_1 and x_2 as zero, we get simulation of the Counter Model in Fig.6. Note that although this model was originally designed to perform the operation instruction like $x_1 + = 1$, values of x_1 and x_2 can both play the role of counter, with only difference in phase.

4. Analysis of Dynamic Behaviours of Universal Oscillator Model

In this section we will explain the choice of parameters of the universal oscillator model in detail and show different dynamic behaviours the model can exhibit.

4.1. Parameters in isolated system $x - y$ and $u - v$

Let's firstly focus on system (9). The function $f(x)$ actually refers to critical manifold S mentioned in section III, small enough ϵ results in different timescales between x and y , which is foundation of analysis on relaxation oscillation. We choose $f(x)$ as a S-shaped function[24] that lies in the first quadrant and the critical manifold S has a unique intersection with the straight line $x + \mu y + \lambda$ on its middle segment i.e. the manifold S_m . We find that the structure in this form is general [24, 23] and has its biochemical correspondence such as the FitzHugh-Nagumo system and the Oregonator model [28]. While in Example 3.3, we use

cubic function to act as function $f(x)$ not only because polynomials are directly related to mass-action kinetics, but also in order to demonstrate the generality of our oscillator model. Note that the parameter ρ should be between the two fold points of $f(x)$ i.e. $1 < \rho < 3$ for existence of relaxation oscillation, and if the equilibrium point of system $x - y$ lies close enough to the fold points $((1, 1)$ and $(3, 5)$ in Example 3.3), then there will be complex oscillations such as canard exposition and mixed-mode oscillation [29], which are not what we want. So we choose $1 < \rho < 3$ and let ρ keep some distance with the two endpoint values.

Then in system $u - v$, isolate this system from system $x - y$ and assume that x in the expression of $\frac{dv}{dt}$ is constant. When the value of parameter c is large enough, u and v actually output the truncated subtraction between the value p and x .

Lemma 4.1 *Assume parameter c is large enough, then the system $u - v$ converges to the following approximate equilibrium depend on the magnitude of x and p :*

$$u = \begin{cases} p - x, & \text{if } p > x \\ 0, & \text{otherwise} \end{cases}$$

$$v = \begin{cases} 0, & \text{if } p > x \\ x - p, & \text{otherwise} \end{cases}$$

Proof *The equilibrium of this system actually expresses as $p - u - cuv = 0$ and $x - v - cuv = 0$. After a simple substitution, we get $v^2 + (p - x + \frac{1}{c})v - \frac{x}{c} = 0$. Since the value of c is large enough, we can simplify it into $v^2 + (p - x)v = 0$, which has two solutions as $v = 0$ and $v = x - p$, corresponding to the magnitude of x and p . Situation of u is similar. ■*

Give x back to oscillator as relaxation oscillation, how u and v follow the periodic oscillation of x to produce similar periodic behaviour depends not only on equilibrium of the isolated system $u - v$ with constant x , but also convergence speed of u and v . Actually, equilibrium can just tell us the long term behaviour of an ODE system, while the periodic change in u and v is a real-time response to oscillation of input x . So restrict to the isolated system $u - v$, we first give a lemma on its exponential convergence:

Lemma 4.2 *For the isolated system $u - v$ as follows:*

$$\frac{du}{dt} = \eta_2(p - u - cuv),$$

$$\frac{dv}{dt} = \eta_2(x - v - cuv).$$
(12)

Parameter p and x are positive constant and different from each other, $\eta_2 > 0$, $c > 0$ and c is large enough. Then the system converges to approximate equilibrium $(p - x, 0)$ or $(0, x - p)$ at exponential speed.

Proof *The approximate equilibrium is shown in Lemma 4.1, we just focus on exponential convergence of this system. It is*

obvious that $u - v$ converges to $p - x$ at exponential speed for that $\frac{d(u-v)}{dt} = \eta_2((p - x) - (u - v))$. Then we can find $k > 0$ and $\lambda > 0$ satisfying $|(u - v) - (p - x)| < ke^{-\lambda t}$ i.e. $(p - x) - u - ke^{-\lambda t} < -v < (p - x) - u + ke^{-\lambda t}$. Substitute into expression of $\frac{du}{dt}$, we get

$$\frac{du}{dt} < \eta_2(p - u - cu^2 + c(p - x)u + cke^{-\lambda t}u)$$

$$< \eta_2(-cu^2 + (c(p - x) + ck - 1)u + p).$$
(13)

Without loss of generality, we only consider the case $p > x$ ($p < x$ is similar). Then for following system:

$$\frac{du}{dt} = \eta_2(-cu^2 + (c(p - x) + ck - 1)u + p),$$

where $-c < 0$, $(c(p - x) + ck - 1) > 0$, $p > 0$, function in the right of the ODE must have two zero roots which we name as u_1 and u_r , and $u_1 < 0 < u_r$ (A large enough c makes the left root u_1 close to zero). Then ODE above can be transformed into

$$\frac{du}{dt} = -c\eta_2(u - u_1)(u - u_r),$$
(14)

which has solution as $u = u_r + \frac{u_r - u_1}{me^{-c(u_1 - u_r)\eta_2 t} - 1}$. So ODE(14) converges to $u = u_r$ at exponential speed. Then ODE $\frac{du}{dt} = \eta_2(p - u - cuv)$ also has exponential convergence by inequality (13). Same for the convergence of v . ■

Expression at equilibrium of u and v is actually our requirement for clock signal in one period. To alternate the values of u and v , we must choose p between high and low amplitudes of oscillator x . In Example 3.3, high amplitude of x is between 4 and 3, while the low amplitude is between 0 and 1, so the range of p is between 1 and 3. Fix the other parameters and choose $p = 0.5$, $p = 2.5$, $p = 3.5$, it is obvious that when p falls out of the range, oscillations of u and v occur in intersecting segments that are not both zero, which destroy the symmetry of u and v as Fig.7.

Based on $p = 2$, we also try different choices of parameter c as 4 and 40. As we emphasize in Lemma 4.1, small value of c would take u and v away from zero at their low amplitudes. For our symmetric clock signals, $c = 400$ is enough.

4.2. Parameters for coupling

In system (9) we introduce η_1 and η_2 which we name 'parameters for coupling'. Role of these parameters is not only to adjust convergence speed and oscillation period of the isolated system, but also resulting in different timescales between these systems when coupling.

Specifically, in system (9), parameter η_1 does not destroy structure of the critical manifold and equilibrium, so amplitude of oscillator x is independent with η_1 . However, η_1 affects the rate of change in x , which is closely related to oscillation period. We choose $\eta_1 = 0.01$ in Example 3.3 in order to magnify period of x and control system $x - y$ on a slower timescale than system $u - v$. While η_2 adjusts period

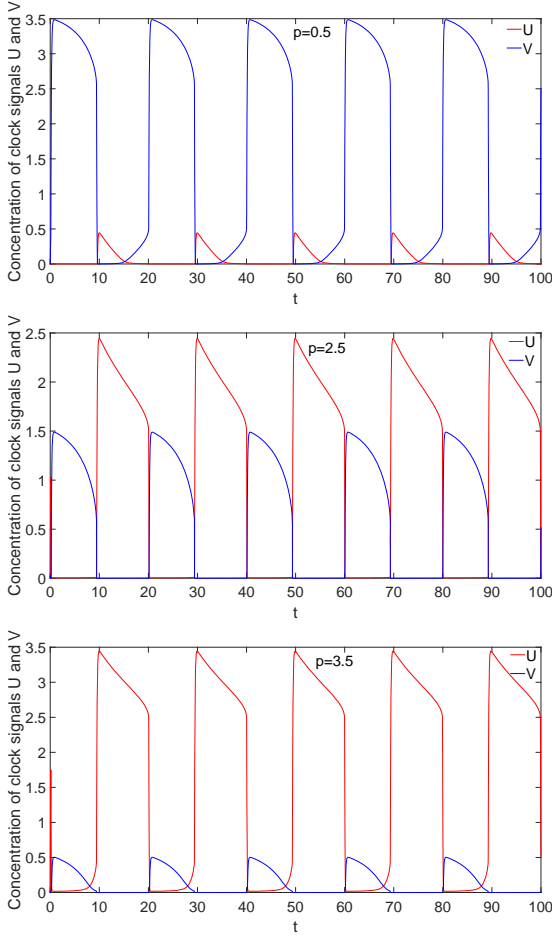


Figure 7: Simulation for $p = 0.5$, $p = 2.5$ and $p = 3.5$.

of the whole system in Example 3.3. We prefer η_2 to be large to speed up the convergence of u and v , which ensures that u and v switch between high and low amplitudes in the form of phase mutations.

Till now, we conclude the choice of parameters and give a theorem that system (9) can act as a universal oscillator model to build a pair of symmetric clock signal U and V as we want.

Theorem 4.1 For system (9), we choose function $f(x)$ and $x + \mu y + \lambda$ as what Theorem 3.1 states. Parameter p is between the fold values of $f(x)$ i.e. $x_m < p < x_M$, c is large enough. η_1 is as small as possible while η_2 is as large as possible. Then for any initial point (x_0, y_0, u_0, v_0) satisfying $x_0 > 0$, $y_0 > 0$, $u_0 \geq 0$ and $v_0 \geq 0$ except for the case that (x_0, y_0) is the unique equilibrium of system $x - y$, oscillation of u and v would exhibit a certain symmetry i.e. corresponding species U and V are pair of symmetric clock signals as Definition 2.4 describes.

Proof As we emphasize in Theorem 3.1 and Example 3.2, isolated system $x - y$ can result in relaxation oscillation which is independent of initial point in the first quadrant of phase plane except for the equilibrium. The equilibrium of isolated system $u - v$ is shown in Lemma 4.1 that when

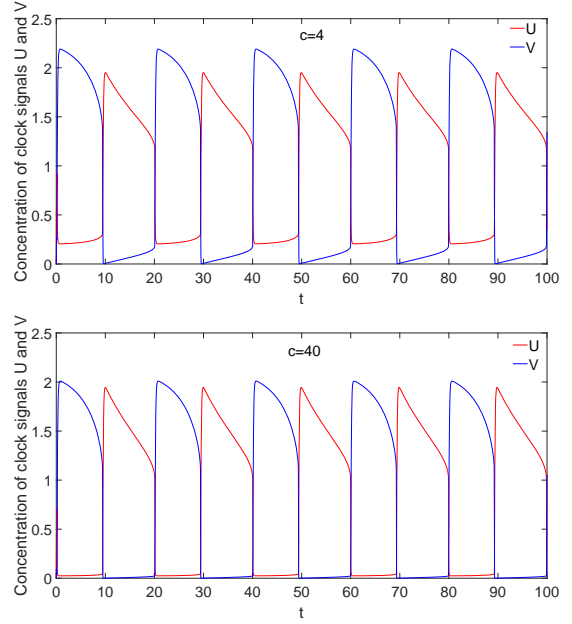


Figure 8: Simulation for $c = 4$ and $c = 40$.

$u = 0, v > 0$, and vice versa. Exponential convergence of the isolated system $u - v$ given by Theorem 4.1, along with small enough η_1 and large enough η_2 makes sure that (u, v) can converge quite quickly to corresponding equilibrium as the value of x changes. So transform system (9) back into chemical reaction networks, species U and V are symmetric clock signals. ■

Moreover, parameter choice in Theorem 4.2 almost erases the response time of u and v with respect to the change in x , so we utilize the period of x to roughly estimate the period of u and v . Imitate approach in [23], we give a formula for calculating the period of x at high amplitude and low amplitude in system (9) as Theorem 4.2.

Theorem 4.2 Consider the relaxation oscillation orbit Γ_ϵ in system $x - y$ of system (9), the period of x i.e. time it takes to travel around the closed orbit Γ_ϵ can be approximated at the first order in ϵ by $T_1 + T_2 + O(1)$ with

$$T_1 = \int_{x_A}^{x_m} \frac{(f'(x) - \frac{d\psi_1}{dx}(x, \epsilon))dx}{\eta_1 \eta_2 (x + \mu(f(x) - \psi_1(x, \epsilon)) + \lambda)(f(x) - \psi_1(x, \epsilon))}, \quad (15)$$

$$T_2 = \int_{x_C}^{x_M} \frac{(f'(x) + \frac{d\psi_2}{dx}(x, \epsilon))dx}{\eta_1 \eta_2 (x + \mu(f(x) + \psi_2(x, \epsilon)) + \lambda)(f(x) + \psi_2(x, \epsilon))}, \quad (16)$$

where ψ_1 and ψ_2 are differentiable function defined separately on $(x_A, x_m) \times (0, \epsilon_0)$ and $(x_C, x_M) \times (0, \epsilon_0)$, and $\exists \xi(\epsilon) = O(\epsilon^{2/3})$, such that

$$\forall x \in (x_A, x_m), |\psi_1(x, \epsilon)| < \xi(\epsilon), \quad (17)$$

$$\forall x \in (x_M, x_C), |\psi_2(x, \epsilon)| < \xi(\epsilon), \quad (18)$$

ϵ_0 is small enough.

Proof We first confirm the formula for T_1 . Lemma 3.1 declares the existence of closed orbit Γ_ϵ which is actually the trajectory of relaxation oscillation, and Γ_ϵ lies in the neighborhood of $O(\epsilon^{2/3})$ of Γ by Fenichel Slow Manifold Theorem. Trajectory Γ in the non-horizontal segment is depicted by critical manifold i.e. $y = f(x)$ in phase plane. Segment of Γ_ϵ closed to $(x, f(x)) : x_A < x < x_m$ is defined as $\Gamma_{\epsilon,l}$:

$$\Gamma_{\epsilon,l} : y = \chi^-(x, \epsilon). \quad (19)$$

So for small enough $\epsilon_0, \forall \epsilon \in (0, \epsilon_0), \exists$

$$\psi_1 : (x, \epsilon) \rightarrow f(x) - \chi^-(x, \epsilon). \quad (20)$$

It is obvious that $\psi_1 > 0$ and is differentiable w.r.t x , and $|\psi_1(x, \epsilon)| < O(\epsilon^{2/3})$ for $\forall x \in (x_A, x_m)$. Then we can substitute $y = f(x) - \psi_1$ into $\frac{dy}{dt}$ in system (9) and get:

$$\begin{aligned} \frac{dy}{dx} &= f'(x) - \frac{d\psi_1}{dx}, \\ \frac{dy}{dt} &= \eta_1 \eta_2 (x + \mu(f(x) - \psi_1(x, \epsilon)) + \lambda)(f(x) - \psi_1(x, \epsilon)). \end{aligned} \quad (21)$$

The time it takes to travel along $\Gamma_{\epsilon,l}$ is given by

$$\begin{aligned} T_1 &= \int_{\Gamma_{\epsilon,l}} dt = \int_{x_A}^{x_m} \frac{1}{\frac{dx}{dt}} dx = \int_{x_A}^{x_m} \frac{\frac{dy}{dx} dx}{\frac{dy}{dt}} dx \\ &= \int_{x_A}^{x_m} \frac{(f'(x) - \frac{d\psi_1}{dx}(x, \epsilon)) dx}{\eta_1 \eta_2 (x + \mu(f(x) - \psi_1(x, \epsilon)) + \lambda)(f(x) - \psi_1(x, \epsilon))}. \end{aligned} \quad (22)$$

Similar for T_2 i.e. time it takes to travel along $\Gamma_{\epsilon,r}$. Since Γ_ϵ in the horizontal segment corresponds to the phase mutation of x between high and low amplitudes, a whole period of x can be approximated as $T_1 + T_2 + O(1)$. ■

Apply Theorem 4.2 to our Example 3.3, we get estimated period of high amplitude and low amplitude of x with parameters stated before as

$$\begin{aligned} T_1 &= \int_0^1 \frac{10(-3x^2 + 12x - 9)}{(x-2)(-x^3 + 6x^2 - 9x + 5)} dx \approx 10.47, \\ T_2 &= \int_4^3 \frac{10(-3x^2 + 12x - 9)}{(x-2)(-x^3 + 6x^2 - 9x + 5)} dx \approx 9.19. \end{aligned}$$

As claimed before, we directly utilize T_1 and T_2 to estimate the period of u and v at high or low amplitude, which is roughly consistent with the simulation result in Fig.5.

While in system (11), we actually use our clock signals U and V to realize Example 2.3 and insert a new parameter

η_3 into the coupled ODEs. The role of η_3 is to coordinate the timescale between the system (10) generating the clock signals and the reaction modules to be adjusted. This is necessary because there is usually a difference between the period of the clock signal i.e. time given for reaction module to converge to equilibrium and the actual time required for reaction module to converge to equilibrium. We choose $\eta_3 = 0.35$ in this example. While we apply the universal oscillator model (9) to other reaction modules to be ordered, value of η_3 is depend on situation.

5. Spontaneous termination of loop

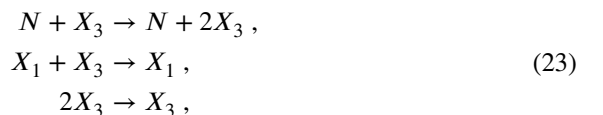
Plenty of studies on chemical oscillators, including previous sections of this paper, mainly focus on implementing the sequential operation of reaction modules, while how to make the system spontaneously terminate the alternate operation of two reaction modules according to certain judgment conditions is also a thought-provoking problem. As we known, oscillation can not end spontaneously, otherwise it would not be an oscillation. So we need to set up additional species to interfere with the loop of reaction modules.

Refer to the computer for setting instructions to jump out of a loop, there are two main methods:

1. One or more variables reaches a specific value;
2. The loop operates for a preset number of times.

The form asks for design according to specific situation, while the latter can be treated in a general way. Come back to our Timer Model as Example 2.3, each time the two modified reaction modules loop, concentration of species X_1 goes up by one(see Fig.6), and concentration of X_1 does not change until the modified reaction module 2 operates again. So the concentration of species X_1 i.e. value of x_1 at any given moment corresponds to the number of loops of these two reaction modules, and by slowing down the frequency of the clock signal U and V , we can use the oscillation period of u and v to refer to the time for one loop of the two reaction modules to be adjusted. When we face two new reaction modules, we add clock signal U and V separately into these modules as catalyst and monitor the number of loops by value of x_1 . For example, when x_1 stabilizes at 100 and is about to jump to 101, the two new reaction modules loop for exactly 100 times.

Next problem is how can the whole system make a spontaneous decision whether to end the loop based on value of x_1 . Our thought also comes from adding catalysts to turn the reaction module on or off. Assume that we need the new reaction modules to loop for n times, then we can build an additional species X_3 which acts as another catalyst of both the two new reaction modules. We just need concentration of X_3 to go to zero when times of loop i.e. value of x_1 increases beyond the preset number n , and this can be realized by a truncated subtraction module as follows:



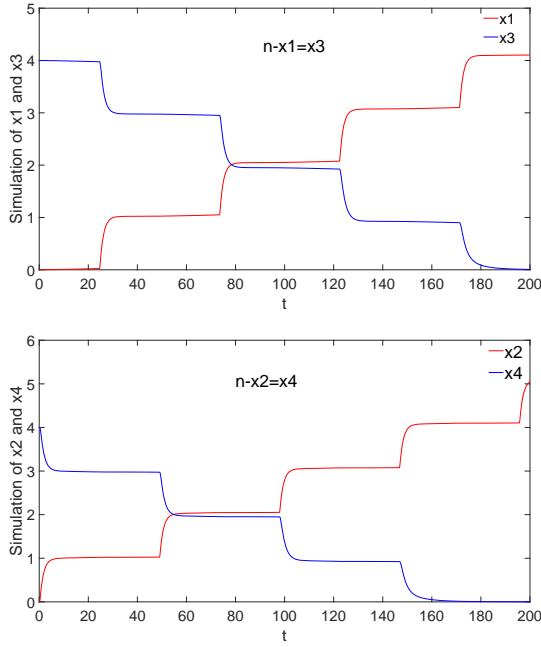


Figure 9: Simulation results of difference operation under dynamic input, with $n=4$.

whose ODE expressed as:

$$\frac{dx_3}{dt} = (n - x_1 - x_3)x_3. \quad (24)$$

We give up the Sub module mentioned in [1] for that the module produces an extra useless species H and exponential convergence of it has not been proven. While in our module (23), exponential convergence is clear:

$$x_3 = \frac{n - x_1}{1 + ke^{-(n-x_1)t}}, k \in \mathbb{R}. \quad (25)$$

So value of x_3 converges to equilibrium at exponential speed and the equilibrium is:

$$x_3 = \begin{cases} n - x_1, & \text{if } n > x_1 \\ 0, & \text{otherwise} \end{cases} \quad (26)$$

Note that if the initial value of x_3 is zero, then it will stay at zero forever. So when we use this module, we can just choose initial value of x_3 as n along with initial value of x_1 equal to zero. Before x_1 goes beyond n , value of x_3 will converge to $n - x_1$ during each loop, and catalyst X_3 always keeps the loop going. When times of loop exceeds the preset number n , x_3 converges quickly to zero, turning both of the two reaction modules off. Couple the ODE (24) with ODEs (11) and keep selection of parameters and initial point unchanged, we get the simulation of x_3 compared with x_1 in Fig.9. We also provide a x_4 as subtraction between the same n and x_2 . We can easily conclude from the simulation diagram that:

1. There is also a phase difference between x_3 and x_4 , which is directly resulted by the phase difference between x_1 and x_2 .

2. The smoothness of x_3 in the descending section is almost equal to the smoothness of x_1 in the ascending section, and the former is affected by both the convergence speed of modified reaction module 2 in Example 2.3 and the convergence speed of our truncated subtraction module (23). So as x_4 .
3. The horizontal segment of x_3 has a slight downward trend, which implies that the horizontal segment of x_1 is not exactly horizontal.

Just from the aim of constructing the Counter Model i.e. building a component whose value increases by one every once in a while, the selection we have given in previous section is enough within acceptable limits of error. When it comes to design of spontaneous termination of loop based on this model, these errors, which could otherwise be ignored, lead to undesirable results. Therefore, in this section, we will consider stricter parameter values.

In our Counter Model, values of both x_1 and x_2 increase periodically over time only with a phase difference. While the increases of x_1 and x_2 calibrate different stages within a single loop: value of component v is firstly positive, leading to the increase of x_2 , then x oscillates at low amplitude and value of u goes strictly beyond zero, resulting in the increase of x_1 . When the roles of u and v are reversed again, one loop is finished. Thus, increase of x_2 happens in beginning of every loop, while increase of x_1 appears in the second half. We'll terminate the loop with components x_3 and x_4 by subtracting x_1 and x_2 with respect to preset loop times n respectively, and demonstrate their effects.

Following example is given by inserting the termination component x_3 back to Counter Model as catalyst to compare the result with Counter model without termination operation.

Example 5.1

$$\begin{aligned} \frac{dx}{dt} &= \eta_1 \eta_2 (-x^3 + 6x^2 - 9x + 5 - y)x/e, \\ \frac{dy}{dt} &= \eta_1 \eta_2 (x - \rho)y, \\ \frac{du}{dt} &= \eta_2 (p - u - cuv), \\ \frac{dv}{dt} &= \eta_2 (x - v - cuv), \\ \frac{dx_1}{dt} &= \eta_3 (x_2 - x_1)u, \\ \frac{dx_2}{dt} &= \eta_3 (x_1 + 1 - x_2)v, \\ \frac{dx_3}{dt} &= \eta_4 (n - x_1 - x_3)x_3, \\ \frac{dx'_1}{dt} &= \eta_5 (x'_2 - x'_1)ux_3, \\ \frac{dx'_2}{dt} &= \eta_5 (x'_1 + 1 - x'_2)vx_3. \end{aligned} \quad (27)$$

We use x'_1 and x'_2 as comparison of x_1 and x_2 under termination component x_3 . In order to reduce the error

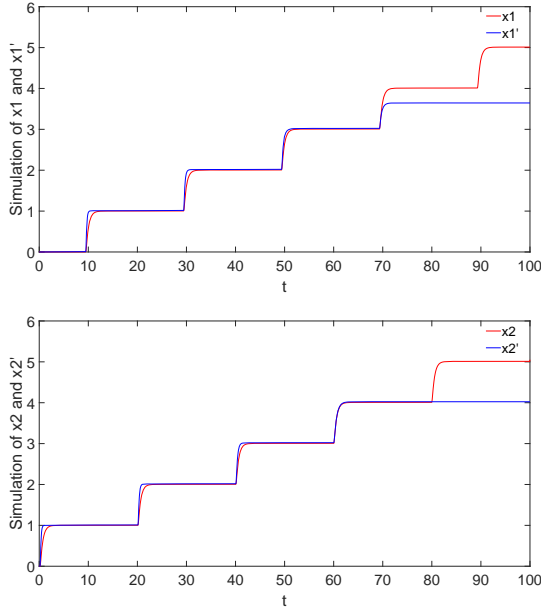


Figure 10: Comparison of x'_1 with x_1 , x'_2 with x_2 under termination component x_3 .

caused by the failure to completely turn the module off at the corresponding time because u and v do not reach zero at their respective low amplitudes, we increase the value of parameter c to 5000. And take η_4 as large as possible to speed up response of x_3 towards changes of x_1 . Let η_3 equal to η_5 for fairness of comparison. In this example, we choose $\epsilon = 0.001$, $\rho = 2$, $p = 2$, $c = 5000$, $n = 4$, $\eta_1 = 0.01$, $\eta_2 = 10$, $\eta_3 = \eta_5 = 1$, $\eta_4 = 500$, and get the simulation in Fig.10.

We also offer Example 5.2 utilizing x_4 as termination component and give corresponding simulation result under the same selection of parameters in Fig.11.

Example 5.2

$$\begin{aligned}
 \frac{dx}{dt} &= \eta_1 \eta_2 (-x^3 + 6x^2 - 9x + 5 - y)x/\epsilon, \\
 \frac{dy}{dt} &= \eta_1 \eta_2 (x - \rho)y, \\
 \frac{du}{dt} &= \eta_2 (p - u - cuv), \\
 \frac{dv}{dt} &= \eta_2 (x - v - cuv), \\
 \frac{dx_1}{dt} &= \eta_3 (x_2 - x_1)u, \\
 \frac{dx_2}{dt} &= \eta_3 (x_1 + 1 - x_2)v, \\
 \frac{dx_4}{dt} &= \eta_4 (n - x_2 - x_4)x_4, \\
 \frac{dx'_1}{dt} &= \eta_5 (x'_2 - x'_1)ux_4, \\
 \frac{dx'_2}{dt} &= \eta_5 (x'_1 + 1 - x'_2)vx_4.
 \end{aligned} \tag{28}$$

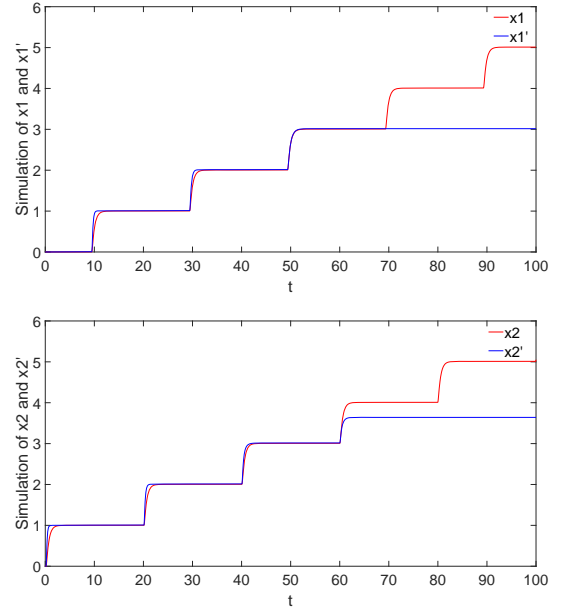


Figure 11: Comparison of x'_1 with x_1 , x'_2 with x_2 under termination component x_4 .

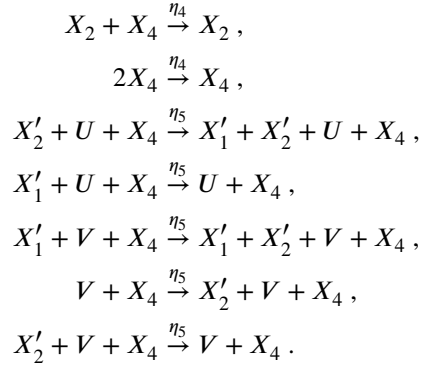
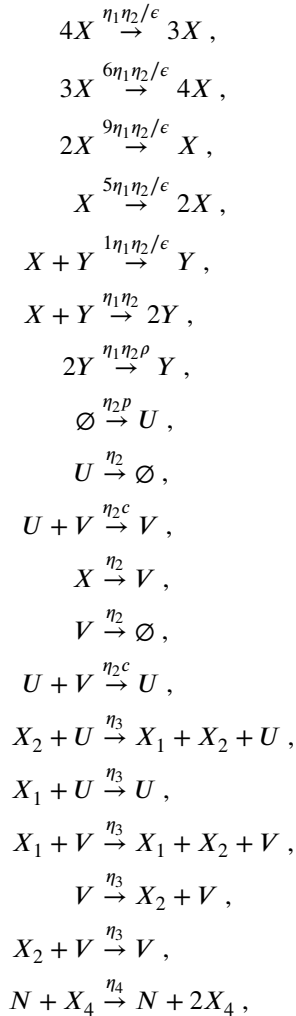
Different choices of termination component contribute to different simulation results of loop termination. Specifically, when using truncated subtraction of preset n and x_1 i.e. x_3 as termination component, change of x_3 happens after x_1 increases by one, which is corresponding to the beginning of second half in one loop. So with preset loop times $n = 4$, after the instruction $x'_1 + = 1$ operates for three times, $x'_1 = x'_2 = 3$ (See the blue lines in Fig.10), $x_1 = x_2 = 3$ (see the red lines in Fig.10) and $x_3 = 1$. Then the fourth loop happens, during the first half, x_2 and x'_2 increase to 4, while x_1 and x'_1 remain unchanged. At the beginning of the second half, x_1 converges to 4 at exponential speed, x_3 responds immediately to this change (Response speed is controlled by η_4) and converges to zero, which sets the rate of change in x'_1 and x'_2 to zero and terminates the loop of Timer Model based on x'_1 and x'_2 . So in Fig.10, when the loop is ended, x'_2 stays at 4 while x'_1 is between 3 and 4 for that during x_2 converges to 4 and causes change in x_3 , x'_2 is also increasing and the increase of x'_2 is aborted because of annihilation of x_3 . In summary, termination of the loop controlled by x_3 occurs after x_2 increases to the preset $n = 4$, when the fourth loop enters the second half. Mechanism in Example 5.1 terminates loop at the beginning of second half of the n th loop.

While in Example 5.2, we choose x_4 as termination component. When the third loop ends, $x_1 = x_2 = x'_1 = x'_2 = 3$ and $x_4 = 1$. Next time the fourth loop begins, x_2 converges to 4 at exponential speed and quickly x_4 responds to zero, the loop of system $x'_1 - x'_2$ is turned off. So mechanism in this example terminates loop at the beginning of n th loop, which can be seen in Fig.11.

Note that neither x_3 nor x_4 can exactly terminate the loop just as the last loop ends. This default can not be overcome

under our mechanism for that both convergence and response take time, and the time at which our termination component ends the loop always lags behind our ideal time. Although we can weaken this lag by adjusting parameters, we emphasize that termination of loop with such precision is sometimes unnecessary in practice. In our Counter Model, if we just choose x_1 as the role of counter, every time x_1 increases when the loop enters the second half, so ending the loop at the beginning of a new one is enough. As Fig.11 shows, if we just want the loop of system $x'_1 - x'_2$ to operate for n times and output the termination value of x'_1 , we just need to use truncated subtraction $n + 1 - x_2$ as termination component and add it into system $x'_1 - x'_2$ as Example 5.2 demonstrates. Similar cases include judging first and then performing the corresponding operation, such as module comparing output with threshold and module performing weight learning in supervised neural network based on chemical reactions [8], and case where the main computation is concentrated in the second half of the loop. For these situations, our strategy of loop termination as Example 5.2 is effective. While if the main computation is concentrated in the first half of the loop, consider the corresponding strategy in Example 5.1.

We transform the ODEs in the Example 5.2 into the corresponding chemical reaction network using mass-action kinetics, and conclude the section with this.



6. General Process of Placing Oscillator Components into Reaction Modules

Our primary goal in designing chemical oscillator is to achieve efficient molecular computation. Recent attempts to build artificial neural networks in biochemical environments [2, 3, 4, 5, 8, 13] have not only improved the computational power of molecular computers [30], but also helped advance the understanding of how living cells perform complex operations.

There have been many ways to build supervised chemical neural network such as multilayer perceptron model and recurrent neural network, with difference lying in the selection of kinetics and chemical reaction network to realize each step of operation instruction. Most chemical neural networks need to adjust the operation sequence of modules in the process of feed-forward value transmission (For example, the reaction module of the later layer needs to wait for the previous layer to complete the operation before performing the corresponding operation), which can theoretically be solved by setting up multiple sets of oscillators. However, work of Vasic et al. [3] on non-competitive CRNs showed that when selecting a specific chemical reaction network structure, the execution order between different modules in the process of feed-forward value transmission does not affect the results of the output layer. In other words, problem about module execution order, which can be avoided by selection of chemical reactions, is not worth the trouble of designing oscillators. While the problem of setting operation sequence for the feed-forward value transmission module and the weight learning module using back propagation algorithm cannot be avoided, because reactions in these two modules tend to share the same species as reactants, which violates the prerequisite of non-competitive CRNs [3]. In Fig.12, we abstract these two reaction modules separately as feed-forward module and back propagation module, and demonstrate the adjustment of oscillator components to the corresponding reaction module.

We use a similar approach to Example 5.2 to achieve the termination species X_4 . As we emphasize in section V, such a design would make the chemical neural network turn off at the beginning of the $n + 1$ th feed-forward value transmission process after a preset number n loops between the feed-forward process and back propagation process. The feed-forward process does not change the weight values, so

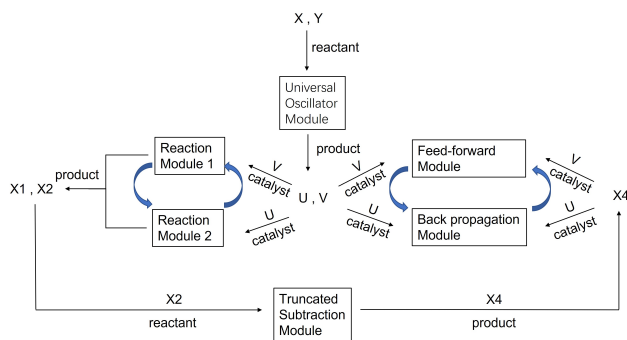


Figure 12: Flow chart of placing oscillator components into reaction modules

the lag of our model for loop termination is irrelevant for training supervised chemical neural network.

Note that only X and Y of the species involved in our oscillator model require strictly given non-zero initial concentration, and the initial concentration of X and Y determines the initial phase of U and V . In Example 3.2, we select specific expression of relaxation oscillation, and let the corresponding initial point be $(x, y) = (1, 1)$. This ensures that V enters the non-zero phase before U (in Fig.5), so we put clock signal V into the module that needs to be prioritized i.e. Feed-forward Module in Fig.12. We can choose the initial concentration of X and Y flexibly according to actual needs, which is also the advantage of our oscillator model. Meanwhile, we prefer initial concentration of X_4 equal to the preset number n to avoid unnecessary error in loop termination.

Although we demonstrate the process of placing oscillator components into the modules with form of flow chart in Fig.12, all of the reactions involved are not constrained by artificial segregation. After we set the initial concentration for all of the species in the system, reaction modules operate in turn due to the concentration change of oscillator components, rather than human intervention. Such design helps simulate more autonomous molecular computation.

7. Conclusion and Discussions

In this paper we develop a systematic approach to realize synchronous sequential computation with abstract chemical reactions. Our ultimate goal is to embed complex calculations into biochemical environments, and after setting the initial values of species and reaction rates, the biochemical system could run automatically to complete the target calculation task. We set up a universal chemical oscillator structure to solve the problem of how to stagger the previously disorderly reactions to make these reactions happen in the order we want. Much of the previous work mentioning chemical oscillators followed the logic of usability, how the oscillation is generated, how it is controlled by the model parameters and how the setting of initial values affects the oscillation properties are not involved in these work [8, 1, 10]. While theoretical analysis of the models and

mechanisms that cause oscillations is improving day by day [28, 24, 23], it is feasible in theory to design transparent chemical oscillators according to actual needs. Inspired by this, we give a universal approach of designing chemical oscillators to control the sequence of two reaction modules.

Different from the harmonic oscillators used in previous work [8, 10], we choose relaxation oscillation as underlying structure of our oscillator model for that mechanism of relaxation oscillation is clear and it is robust independent to initial points. While existence and property of harmonic oscillators are depend on the selection of initial point, which is not flexible in response to specific application requirements. Besides, harsh selection of initial points often causes difficulties for biochemical implementation. In our design, parameters and structure of the chemical oscillator can be dynamically adjusted according to the needs of actual use, and to some extent, it is our oscillator model that adapts to the actual needs, rather than the other way around.

We explore the steps of building oscillator model and generating pair of symmetric clock signals, and give a simple example (Example 3.3) to fulfill our aim. As far as we know, to get a pair of symmetric clock signals, at the level of chemical reaction network theory, requires at least four species. In [10], the authors constructed a reaction network involved 12 species. In [8], to get two clock signals, dimension of the oscillator model is four. Therefore, our oscillator model is concise enough in terms of the number of species used. Selection of $f(x, y)$ in ODEs (4) is also flexible, taking it as a simple cubic function is enough for the rest of design. Tyson and Fife [28] abstracted another expression of $f(x, y)(f(x, y) = x(1 - x) - by(x - a)/(x + a)$, while $g(x, y) = x - y$, a and b are parameters) according to real chemical reactions. Substituting this set of structure, our oscillator model is still usable.

Although our analysis of the model mainly focus on the ODE level, we still fully consider its correspondence with chemical reactions when building the ODE model. Only when we set up the model for triggering relaxation oscillation, we do not specifically select ODE structures directly related to chemical reactions because models abstracted from biochemical examples are often too complex for theoretical analysis. Designs of other steps are derived directly from abstract chemical reactions, based on the principle that deterministic chemical kinetics is Turing universal [15]. We turn a whole example (Example 5.2) into abstract chemical reaction network at the end of section V, embedding additional parameters we introduce in rate constants of the corresponding reactions. Our analysis ends with the ODE simulation and the corresponding abstract chemical reaction network, while the subsequent work such as transform these abstract reactions into chemistry, can be achieved by DNA strand displacement cascades, which is beyond the scope of this paper.

We tested the effect of our oscillator model under the Counter Model, which can basically achieve the purpose we want. While faced with more complicated task, such as designing reaction sequences for the modules of a complete

biochemical feed-forward neural network, Our oscillator models actually function as hubs: combining and splicing the reaction modules to achieve a complete operation. Although this task is implemented in the same way that we realize the simple instruction $x_1 + = 1$, implementation of a whole biochemical feed-forward neural network is much more difficult and consists of large number of parameters to be analyzed. In the future we will do further analysis on implementing such more complex calculations.

Note that selection of parameters could arise dynamic behaviour as we want, our model is not as accurate as it looks, yet. We choose parameter c and η_4 as large as possible in order to turn the low amplitude of u and v close enough to zero and accelerate the convergence speed. Limited by what we know about oscillations, we can only do so much. Other work such as [8] is also a similar process to make the result look perfect. We think it's more reasonable to apply those constraints to reaction rate constants than to pick harshly selected initial values of species.

Different from previous perspectives, we believe that how to make the system spontaneously terminate loops controlled by clock signals is also an important topic, and we give a feasible method to tackle with this that works in some situations. While as we emphasize in section V, our idea of ending loops is not universal for that our design does not allow the whole system to spontaneously turn off the entire loop at the end of the n th loop. This is because the termination component itself needs to respond to the new loop and then close it, and the resulting lag cannot be overcome by the model itself. We've tried other approaches, such as setting a module that performs the Sigmoid function to dynamically set the termination component to zero or one, which still fail to overcome the lag and increase the complexity of model. How to make our loop termination strategy more efficient is also a problem for future.

Our work provides theoretical analysis and assurance for embedding efficient algorithms in fields such as machine learning into biochemical environments, and oscillation plays an indispensable role in it. Different from modeling and analyzing the oscillations observed in biochemical experiments, it is also an attractive research content to design models to achieve the desired functions based on the understanding of oscillation. Recently, there has also been some work to build machine learning algorithms using oscillations. In [31, 32], the authors designed new structure of recurrent neural network and graph neural network based on coupled oscillators. how oscillations and the knowledge within the field of dynamical systems associated with oscillations, can serve other fields such as molecular computing and machine learning, will also be the focus of our future research.

References

- [1] M. Vasić, D. Soloveichik, S. Khurshid, Crn++: Molecular programming language, *Natural Computing* 19 (2020) 391–407.
- [2] A. Moorman, C. C. Samaniego, C. Maley, R. Weiss, A dynamical biomolecular neural network, in: 2019 IEEE 58th Conference on Decision and Control (CDC), IEEE, 2019, pp. 1797–1802.
- [3] M. Vasic, C. Chalk, A. Luchsinger, S. Khurshid, D. Soloveichik, Programming and training rate-independent chemical reaction networks, arXiv preprint arXiv:2109.11422 (2021).
- [4] H.-J. K. Chiang, J.-H. R. Jiang, F. Fages, Reconfigurable neuro-morphic computation in biochemical systems, in: 2015 37th Annual International Conference of the IEEE Engineering in Medicine and Biology Society (EMBC), IEEE, 2015, pp. 937–940.
- [5] D. Blount, P. Banda, C. Teuscher, D. Stefanovic, Feedforward chemical neural network: An in silico chemical system that learns xor, *Artificial life* 23 (2017) 295–317.
- [6] J. J. Tyson, *The belousov-zhabotinskii reaction*, volume 10, Springer Science & Business Media, 2013.
- [7] D. B. Forger, *Biological clocks, rhythms, and oscillations: the theory of biological timekeeping* (2017).
- [8] D. Arredondo, M. R. Lakin, Supervised learning in a multilayer, nonlinear chemical neural network, *IEEE Transactions on Neural Networks and Learning Systems* (2022).
- [9] M. Lachmann, G. Sella, The computationally complete ant colony: Global coordination in a system with no hierarchy, in: *European Conference on Artificial Life*, Springer, 1995, pp. 784–800.
- [10] H. Jiang, M. Riedel, K. Parhi, Synchronous sequential computation with molecular reactions, in: *Proceedings of the 48th Design Automation Conference*, 2011, pp. 836–841.
- [11] M. Feinberg, *Foundations of chemical reaction network theory* (2019).
- [12] D. Soloveichik, G. Seelig, E. Winfree, Dna as a universal substrate for chemical kinetics, *Proceedings of the National Academy of Sciences* 107 (2010) 5393–5398.
- [13] D. F. Anderson, B. Joshi, A. Deshpande, On reaction network implementations of neural networks, *Journal of the Royal Society Interface* 18 (2021) 20210031.
- [14] H. Buisman, H. M. ten Eikelder, P. A. Hilbers, A. M. Liekens, Computing algebraic functions with biochemical reaction networks, *Artificial life* 15 (2009) 5–19.
- [15] F. Fages, G. L. Guludec, O. Bournez, A. Pouly, Strong turing completeness of continuous chemical reaction networks and compilation of mixed analog-digital programs, in: *International conference on computational methods in systems biology*, Springer, 2017, pp. 108–127.
- [16] C. Chalk, N. Kornerup, W. Reeves, D. Soloveichik, Composable rate-independent computation in continuous chemical reaction networks, *IEEE/ACM Transactions on Computational Biology and Bioinformatics* 18 (2019) 250–260.
- [17] D. Gonze, P. Ruoff, The goodwin oscillator and its legacy, *Acta Biotheoretica* 69 (2021) 857–874.
- [18] M. Banaji, Inheritance of oscillation in chemical reaction networks, *Applied Mathematics and Computation* 325 (2018) 191–209.
- [19] C. Conradi, M. Mincheva, A. Shiu, Emergence of oscillations in a mixed-mechanism phosphorylation system, *Bulletin of mathematical biology* 81 (2019) 1829–1852.
- [20] I. R. Epstein, J. A. Pojman, *An introduction to nonlinear chemical dynamics: oscillations, waves, patterns, and chaos*, Oxford university press, 1998.
- [21] M. Krupa, A. Vidal, F. Clément, A network model of the periodic synchronization process in the dynamics of calcium concentration in gnRH neurons, *The Journal of Mathematical Neuroscience* 3 (2013) 1–24.
- [22] R. J. Field, R. M. Noyes, Oscillations in chemical systems. iv. limit cycle behavior in a model of a real chemical reaction, *The Journal of Chemical Physics* 60 (1974) 1877–1884.
- [23] S. Fernández-García, A. Vidal, Symmetric coupling of multiple timescale systems with mixed-mode oscillations and synchronization, *Physica D: Nonlinear Phenomena* 401 (2020) 132129.
- [24] M. Krupa, P. Szmolyan, Relaxation oscillation and canard explosion, *Journal of Differential Equations* 174 (2001) 312–368.
- [25] J. Grasman, *Asymptotic methods for relaxation oscillations and applications*, volume 63, Springer Science & Business Media, 2012.

- [26] N. Fenichel, Geometric singular perturbation theory for ordinary differential equations, *Journal of differential equations* 31 (1979) 53–98.
- [27] K. Hangos, G. Szederkényi, Mass action realizations of reaction kinetic system models on various time scales, in: *Journal of Physics: Conference Series*, volume 268, IOP Publishing, 2011, p. 012009.
- [28] J. J. Tyson, P. C. Fife, Target patterns in a realistic model of the belousov–zhabotinskii reaction, *The Journal of Chemical Physics* 73 (1980) 2224–2237.
- [29] M. Wechselberger, Existence and bifurcation of canards in \mathbb{R}^3 in the case of a folded node, *SIAM Journal on Applied Dynamical Systems* 4 (2005) 101–139.
- [30] Y. Benenson, B. Gil, U. Ben-Dor, R. Adar, E. Shapiro, An autonomous molecular computer for logical control of gene expression, *Nature* 429 (2004) 423–429.
- [31] T. K. Rusch, S. Mishra, Coupled oscillatory recurrent neural network (cornn): An accurate and (gradient) stable architecture for learning long time dependencies, *arXiv preprint arXiv:2010.00951* (2020).
- [32] T. K. Rusch, B. P. Chamberlain, J. Rowbottom, S. Mishra, M. M. Bronstein, Graph-coupled oscillator networks, *arXiv preprint arXiv:2202.02296* (2022).